IMPULSIVE PHASE OF FLARES IN SOFT X-RAY EMISSION

E. ANTONUCCI[1]*, A. H. GABRIEL[1], L. W. ACTON[2], J. L. CULHANE[3],
J. G. DOYLE[4], J. W. LEIBACHER[2],
M. E. MACHADO[5], L. E. ORWIG[6], and C. G. RAPLEY[3]

(Received 10 April, in revised form 3 August, 1981)

Abstract. Observations using the Bent Crystal Spectrometer instrument on the Solar Maximum Mission show that turbulence and blue-shifted motions are characteristic of the soft X-ray plasma during the impulsive phase of flares, and are coincident with the hard X-ray bursts observed by the Hard X-ray Burst Spectrometer. A method for analysing the Ca XIX and Fe XXV spectra characteristic of the impulsive phase is presented. Non-thermal widths and blue-shifted components in the spectral lines of Ca XIX and Fe XXV indicate the presence of turbulent velocities exceeding 100 km s^{-1} and upward motions of 300–400 km s^{-1}.

The April 10, May 9, and June 29, 1980 flares are studied. Detailed study of the geometry of the region, inferred from the Flat Crystal Spectrometer measurements and the image of the flare detected by the Hard X-ray Imaging Spectrometer, shows that the April 10 flare has two separated footpoints bright in hard X-rays. Plasma heated to temperatures greater than 10^7 K rises from the footpoints. During the three minutes in which the evaporation process occurs an energy of 3.7×10^{30} ergs is deposited in the loop. At the end of the evaporation process, the total energy observed in the loop reaches its maximum value of 3×10^{30} ergs. This is consistent with the above figures, allowing for loss by radiation and conduction. Thus the energy input due to the blue-shifted plasma flowing into the flaring loop through the footpoints can account for the thermal and turbulent energy accumulated in this region during the impulsive phase.

1. Introduction

The Bent Crystal Spectrometer (BCS) of the X-Ray Polychromator experiment was in operation from February 1980 to November 1980 on the Solar Maximum Mission satellite (SMM). The soft X-ray emission in the spectral bands 3.165–3.226 Å and 1.843–1.896 Å, covering respectively the Ca XIX and Fe XXV resonance lines as well as their associated dielectronic satellite lines, has systematically shown the existence of features of the line profiles characteristic of the impulsive phase of solar flares, and temporally coincident with the hard X-ray burst. The line profiles observed early in the flare indicate the dynamic processes of the plasma during the impulsive phase. Turbulent motions in the hot plasma reach velocities higher than 100 km s^{-1} at the peak of the hard X-ray emission (energies > 50 keV), as measured by the Hard X-Ray Burst Spectrometer (HXRBS) on board the SMM satellite, and greatly exceed throughout the impulsive phase the value found in the preflare active region. Upward motions of plasma with vertical velocities of a few hundred km s^{-1} are also observed during the hard X-ray

[1] Space and Astrophysics Division, Rutherford Appleton Laboratory, Chilton, England.
[2] Lockheed Missiles and Space Co., Inc., Lockheed Palo Alto Research Laboratory, U.S.A.
[3] Mullard Space Science Laboratory, University College London, England.
[4] Department of Applied Mathematics and Theoretical Physics, The Queen's University of Belfast, N. Ireland.
[5] Observatorio de Fisica Cosmica – CNIE, San Miguel, Argentina.
[6] NASA Goddard Space Flight Center, Greenbelt, U.S.A.
* On leave from Torino University, Italy.

Solar Physics **78** (1982) 107–123. 0038–0938/82/0781–0107$02.55.

bursts. These are the first observations to correlate soft X-ray line broadenings and blue-shifts with the hard X-ray bursts. The association of line broadenings with the impulsive phase has been reported earlier by Gabriel *et al.* (1981a, b) and Culhane *et al.* (1981), and with the rising phase of flares by Doschek *et al.* (1980), and Feldman *et al.* (1980). Observations of mass motions and turbulence during flares in the transition region and chromosphere are reviewed by Canfield *et al.* (1980). In addition to the hard X-ray, extreme ultraviolet, radio and optical impulsive phenomena, the dynamics of the plasma emitting soft X-rays provides promising new information for the understanding of the energy release process during flares.

2. Analysis of the Soft X-Ray Spectra

The Bent Crystal Spectrometer consists of eight channels producing eight simultaneous spectra in different spectroscopic regions (Acton *et al.*, 1980; Culhane *et al.*, 1981). The dispersed spectra obtained by means of an appropriate crystal curvature are detected by position sensitive proportional counters. A time resolution of 0.128 s can be achieved during intense solar flares although in the present analysis integration times of 9 s or longer have been used. The spectrometers have $6' \times 6'$ (FWHM) collimators, but the effective collimation is produced by the angular size of the bright region observed, normally a flare.

The BCS spectral regions have been optimised to exploit the unique diagnostic capabilities of the group of dielectronic satellite lines situated on the long-wavelength side of the helium-like resonance lines of calcium and iron. Theory for the use of these spectra has been dealt with in a series of publications, notably Bhalla *et al.* (1975), Bely-Dubau *et al.* (1979a, b). Various line ratios within these groups enable the derivation of electron temperature T_e and the ionization ratios of lithium-like to helium-like ions and helium-like to hydrogen-like ions. These quantities allow the determination of the rate of change of ionization balance in the plasma; a quantity of some importance for transient flare analysis.

The theory used for the present analysis includes a number of recent improvements: i.e. new ratios for inner-shell excitation of the lithium-like ions, plus a completely new calculation for the helium-like ion lines, including excitation, cascade, radiative and dielectronic recombination and direct ionization/excitation from the lithium-like ions. These theoretical improvements are all described in recent papers by Bely-Dubau *et al.* (1981, 1982).

Interpretation of observed spectra is complicated by problems associated with the finite widths or profiles of the emitted lines. These profiles are a combination of intrinsic width, due to the Doppler motions of the ions, and instrumental effects, due to rocking curves of the crystals, and in some cases for the BCS, the finite angular size of the source. Since the lines are quite close together, merging occurs in some cases, with the wings of line profiles overlapping. For these reasons, curve fitting techniques have been developed for the analysis, rather than simply measuring the height or area of individual lines.

The technique involves the construction of a synthesised theoretical spectrum derived from a set of trial plasma parameters. This line spectrum is convolved with a Gaussian profile to allow for thermal and random non-thermal motions, and a Lorentzian profile to characterise the crystal response. Finally, this is compared with the observed spectrum after (a) normalising and (b) shifting on a wavelength scale, so that the resonance line coincide. With the help of an interactive video display on a PDP 11/34 mini-computer system, the trial parameters can be adjusted, and by visual assessment one can readily obtain the best fit to the principal diagnostic lines. The parameter-set thus determined includes electron temperature T_e, equivalent ion temperature T_i (which includes thermal and non-thermal effects), Li/He-like ion ratio, H/He-like ion ratio, plus instrumental parameters such as background and crystal rocking-curve. It should be noted that this technique completely compensates for problems of overlapping of spectral line profiles, so long as the theory includes all features contributing to the relevant parts of the spectrum.

Figures 1 and 2 give examples of the degree of accuracy achieved in reproducing the observed spectra. The computed spectra are normalised to the observed ones. The values of the parameters determined by fitting the soft X-ray emission versus wavelength are

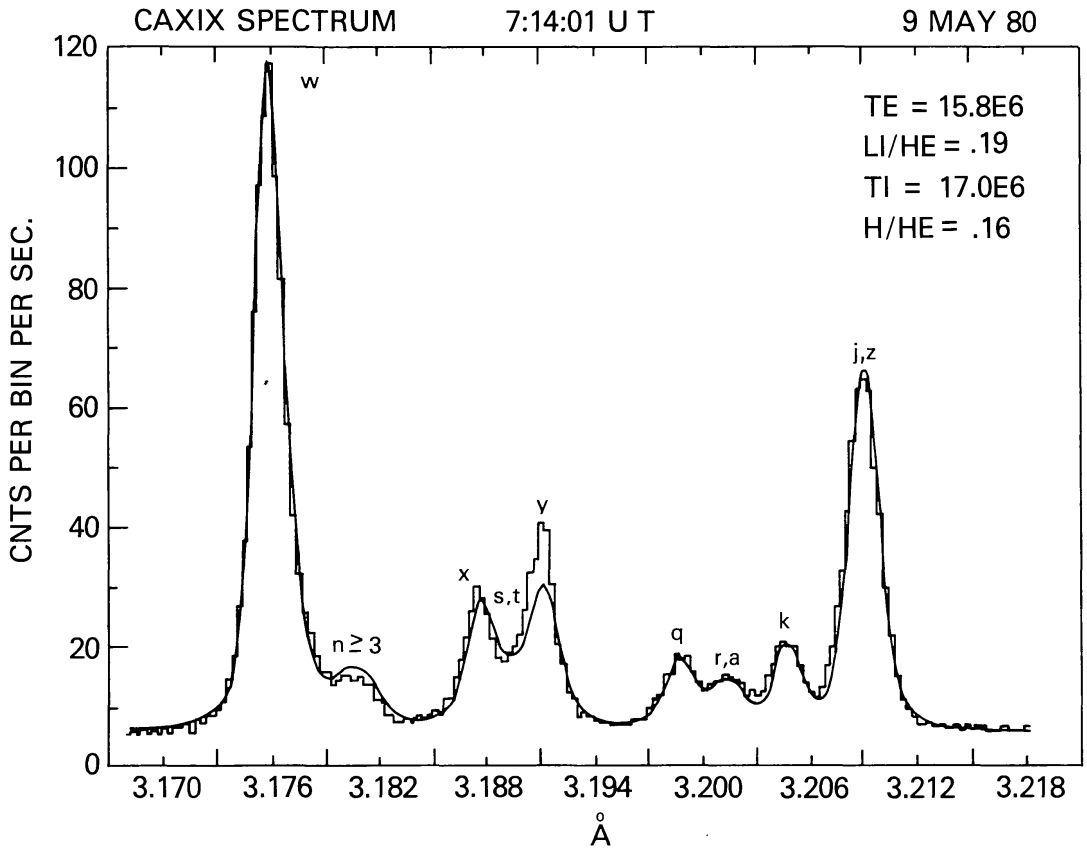

Fig. 1. The Ca XIX BCS spectrum observed at 07 : 14 : 01 UT, May 9, 1980 averaged over 51 s, is compared with the theoretical spectrum for an electron temperature $T_e = 15.8 \times 10^6$ K, an equivalent ion temperature $T_i = 17.0 \pm 2.0 \times 10^6$ K, Li–He-like ion abundance ratio Li/He = 0.19 ± 0.02 and the H–He-like ion abundance ratio H/He = 0.16 ± 0.02. This spectrum is characteristic of the gradual phase of a flare at, or after, the peak of the emission intensity (for T_e errors see text).

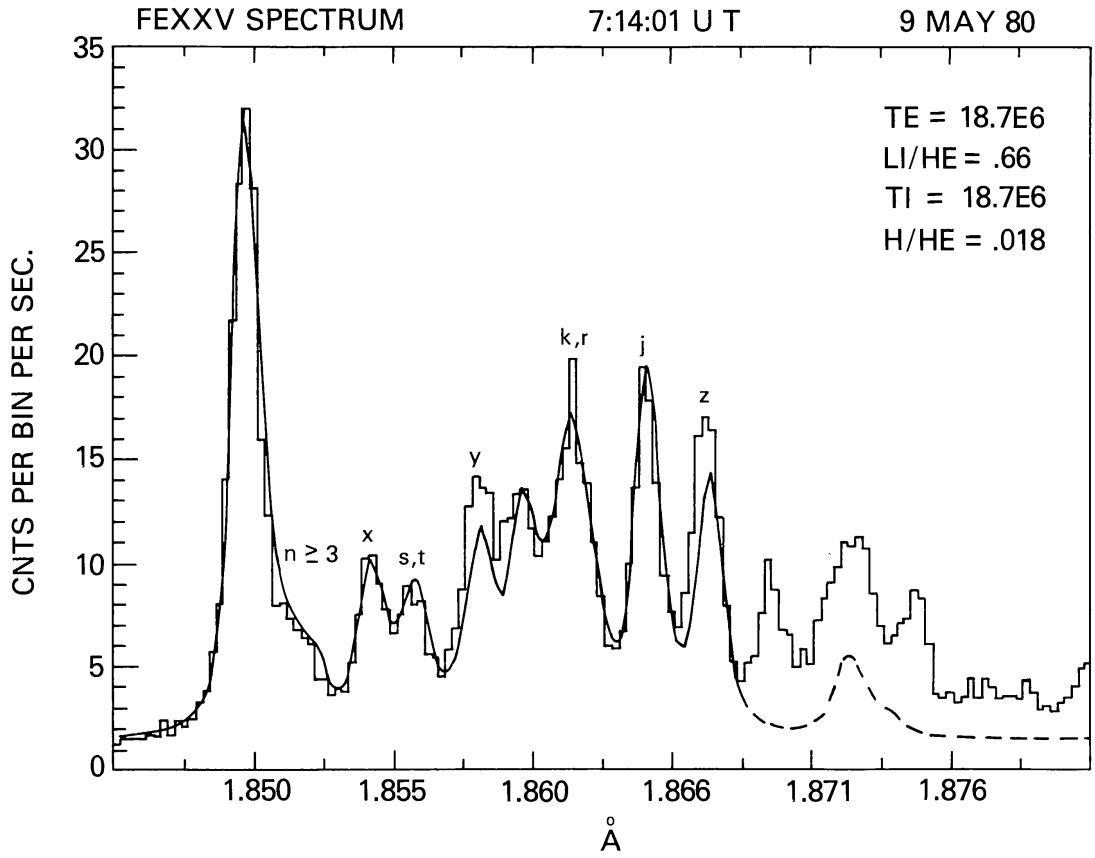

Fig. 2. The Fe XXV BCS spectrum observed at 07 : 14 : 01 UT, May 9, 1980, averaged over 51 s, is compared with the theoretical spectrum for $T_e = 18.7 \times 10^6$ K, $T_i = 18.7 \pm 0.3 \times 10^6$ K, Li/He = 0.66 ± 0.03 and H/He = 0.018 ± 0.003.

also reported. The source responsible for the calcium emission is at a temperature of 1.58×10^7 K. For the iron source an electron temperature of 1.87×10^7 K is found. These measurements are sensitive to small changes of the order of 0.02×10^7 K, although there may be a systematic error of $\sim 10\%$ arising from the atomic data. The line broadening is close to thermal: $T_i = 1.7 \pm 0.2 \times 10^7$ K is found for Ca and $1.87 \pm 0.3 \times 10^7$ K for Fe. The ratios of H-like to He-like and Li-like to He-like ion populations, representative of the ionization state of the plasma and its departure from equilibrium, are reported in Figures 1and 2. In the iron spectrum the intercombination lines appear yet to be underestimated, probably due to the neglect of Fe XXIII satellite lines (Dubau, private communication). For the same reason the theoretical fit is not significant for wavelengths longer than 1.868 Å. The large discrepancy between the observed and theoretical *y* line in the calcium spectrum is of instrumental origin.

The analysis of the time evolution of the soft X-ray emission during a flare event in the two spectral regions considered shows that during the gradual phase the observed spectrum is adequately described at each given time by a single theoretical spectrum as described in Figures 1 and 2. However, during the impulsive phase the resonance line shows systematically a well-defined blue wing, while the whole spectrum appears distorted. This effect is shown in Figure 3. The observations refer to the April 10, 1980,

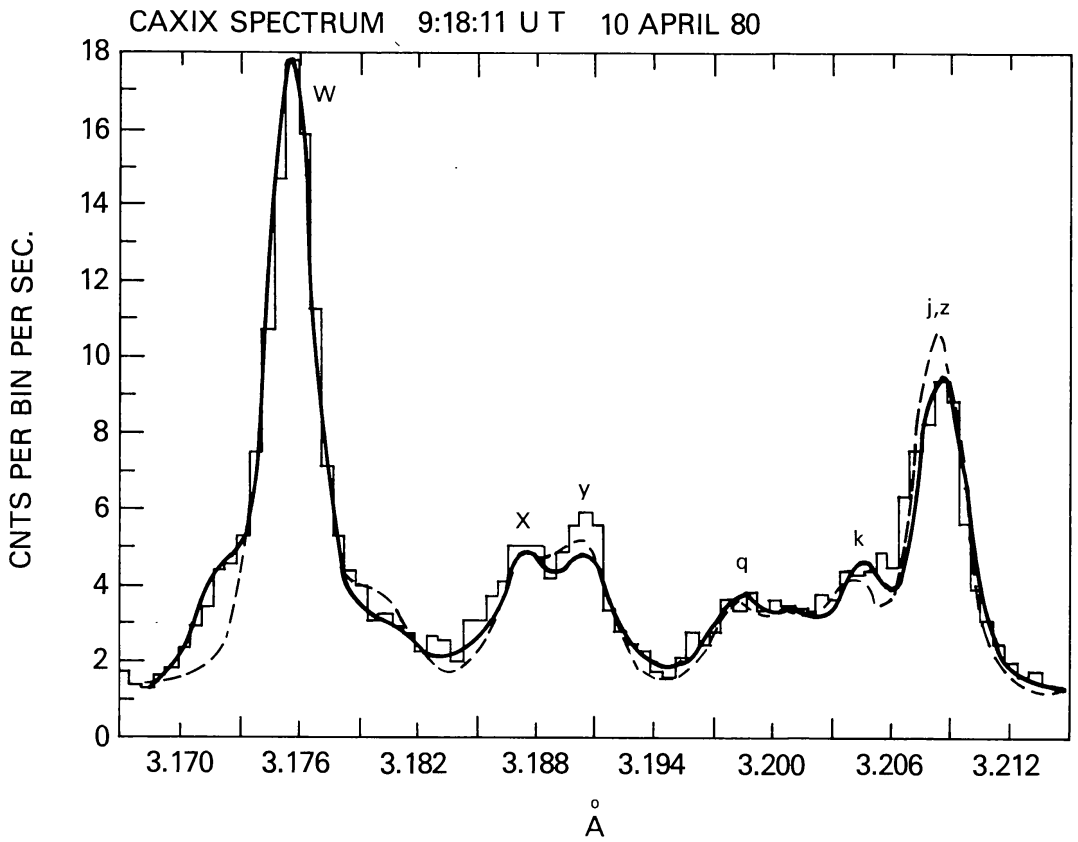

Fig. 3. The Ca XIX BCS spectrum is observed at 09 : 18 : 11 UT during the impulsive phase of the April 10, 1980 flare. This spectrum is a composite of a principal component with non-thermal line width and a blue-shifted secondary component. The best fit is found by superposing two theoretical spectra, the second of which is blue-shifted by 3.6 mÅ and with intensity a factor 0.16 of the first.

flare at 09 : 18 : 11 UT. A single theoretical spectrum (dashed line) is insufficient to reproduce the observed spectral profiles. However, the distorted spectrum observed during the impulsive phase can be easily fitted by superposing two theoretical spectra (secondary one blue-shifted with respect to the principal one), each one defined by a set of adjustable parameters. The calcium spectrum of Figure 3 is reproduced by the superposition of two components (continuous line): the secondary spectrum is shifted to the shorter wavelengths by 3.6 mÅ with respect to the principal one and its intensity is 0.16 of the intensity of the principal component. The electron temperature, ion ratios and equivalent ion temperature of the two superposed spectra are assumed to be the same. This implies that since the ratio of the blue-shifted to the principal spectrum has typical values in the range 0.15–0.30, the physical parameters derived represent reliably only the conditions of the source of the principal component of the soft X-ray emission. That is, the contribution to the main diagnostic lines from the nearby lines at longer wavelengths, due to the blue-shifted component, is taken into account although the dependence of this contribution on the physical parameters of the blue-shifted source (which might be different from the primary X-ray source) is neglected. If one assumed a single-component spectrum the electron temperature would be underestimated. From the two-component fitting the values $T_e = 1.6 \pm 0.04 \times 10^7$ K,

Li/He = 0.24 ± 0.025, and H/He = 0.08 ± 0.03 are derived. The errors quoted represent the precision of fitting and do not include systematic errors. The dashed lines instead representing the single-component fitting would give an electron temperature of $1.32 \pm 0.04\ 10^7$ K and a Li/He ratio equal to 0.25 ± 0.025. Because of the blending of satellite lines, the iron spectrum is much more confused when a blue-shifted component is present, and in this case also, the two-component fitting reproduces the spectral profile much more adequately than the single-component one.

The broadening of calcium lines (Figure 3) corresponds to an equivalent ion temperature $T_i = 4.3 \pm 0.3 \times 10^7$ K, much in excess of thermal broadening ($T_e = 1.6 \times 10^7$ K). For the iron lines in the same time interval, $T_i = 4.8 \pm 0.35 \times 10^7$ K exceeds $T_e = 1.77 \pm 0.06 \times 10^7$ K. Both the broadenings and blue-shifts in soft X-ray emission lines during the impulsive phase will be discussed in the next section.

3. Interpretation of Impulsive Phase in the Soft X-Ray Emission

In the previous section we have pointed out that the spectral lines observed in the early phase of flares show a broadening greatly exceeding the thermal widths and a blue-shifted component in the calcium and iron spectra. Spectral lines, broader during the rise phase than during the decay phase as well as blue-shifts have been observed in previous Ca XIX and Fe XXV spectra (Doschek *et al.*, 1980; Feldman *et al.*, 1980). However, the SOLFLEX experiment provides spectra scanned at a time resolution (56 s) not always sufficient for studying in detail impulsive phenomena. We will now discuss the time correlation of the dynamic phenomena observed in soft X-rays with the hard X-ray bursts detected by the HXRBS on SMM. The time evolution of the soft and hard X-ray emission is studied for three events: the April 10, 1980 flare occurring at 09 : 17 : 00 UT in the active region 2372 at N 12, W 42 (optical importance 1N, X-ray classification M4); the May 9, 1980 flare starting at 07 : 11 : 30 UT in active region 2418 at S21, W32 (1B, M7) and the June 29, 1980 event at 18 : 22 : 00 UT associated with a bright surge at the limb from active region 2522 at S29, W90 (M4). Figures 4, 5, and 6 present for each flare a comparison of the time variation of the electron temperature T_e and equivalent ion temperature T_i, for the principal component of the iron and calcium emission, and the hard X-ray emission at energies > 52 keV. The peak of the major hard X-ray burst is seen to be coincident with the largest excess of non-thermal broadening of the soft X-ray spectral lines, indicating the highest degree of turbulence of the hot plasma at that time.

The April 10 and June 29 flares are particularly suitable for the observation of the onset of the impulsive phase phenomena, since the active region was hot and dense enough to produce significant Ca XIX emission prior to the flares as a consequence of small brightenings occurring respectively at 09 : 06 UT and 18 : 06 UT. In the first case (Figure 4) the non-thermal component of the line widths in the pre-flare active region indicates mean turbulent velocities of the order of 75 km s^{-1}. However in coincidence with the hard X-ray burst, the turbulence increases, reaching its maximum value, 122 km s^{-1}, at the peak of the hard X-ray burst at 09 : 18 : 37 UT (short integration times

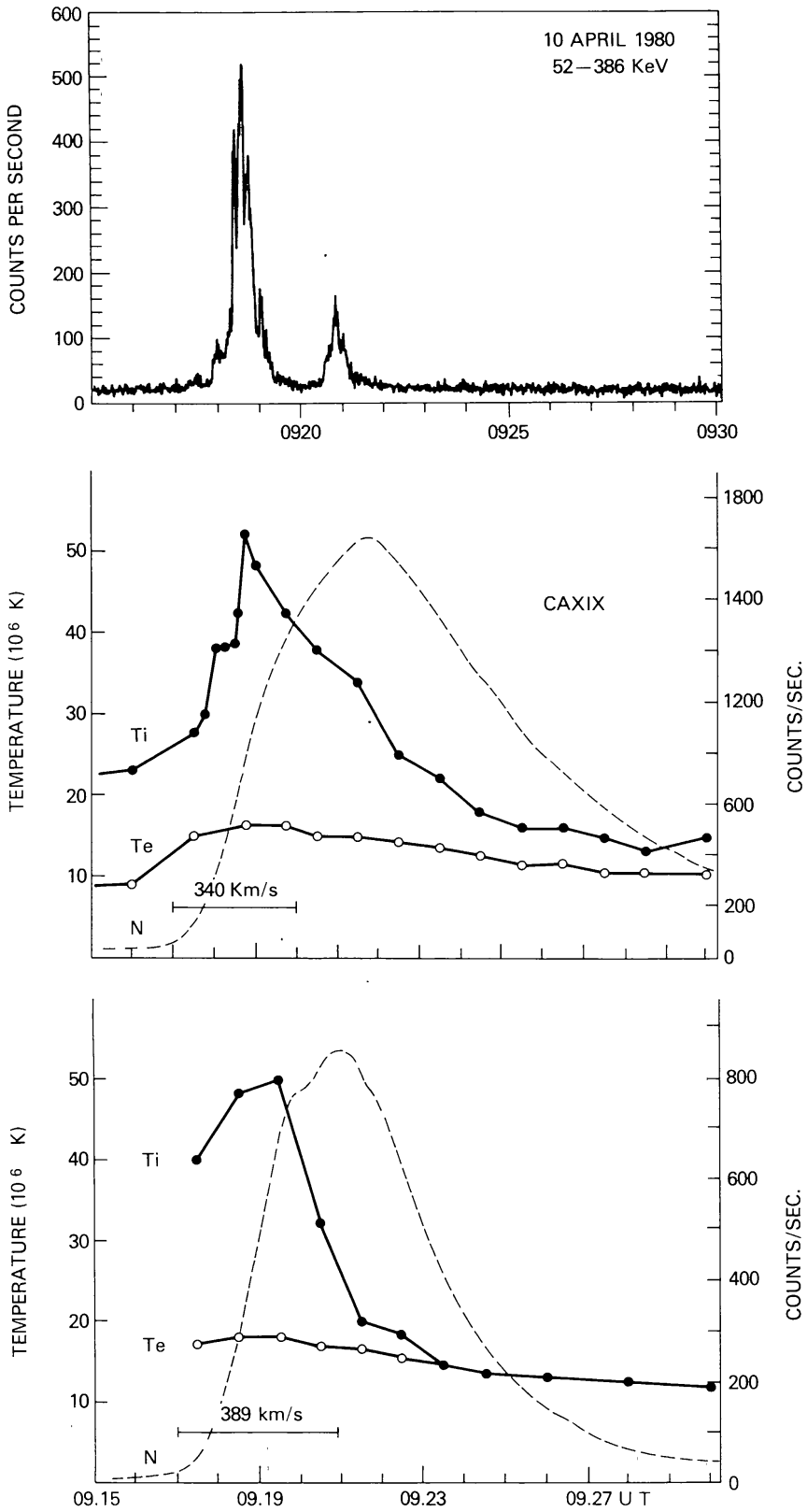

Fig. 4. Hard X-ray emission in the energy band 52–386 keV during the April 10, 1980 flare detected by the HXRBS, at the top of the figure. In the middle, the time profile of the soft X-ray emission N integrated over the whole spectral region of Ca XIX resonance line and satellites, detected by the BCS, is compared with the evolution of the electron temperature T_e and the equivalent ion temperature T_i. The period in which upward velocities are present is indicated by the horizontal bar as well as their highest value. At the bottom the same parameters are plotted, derived from the Fe XXV spectra.

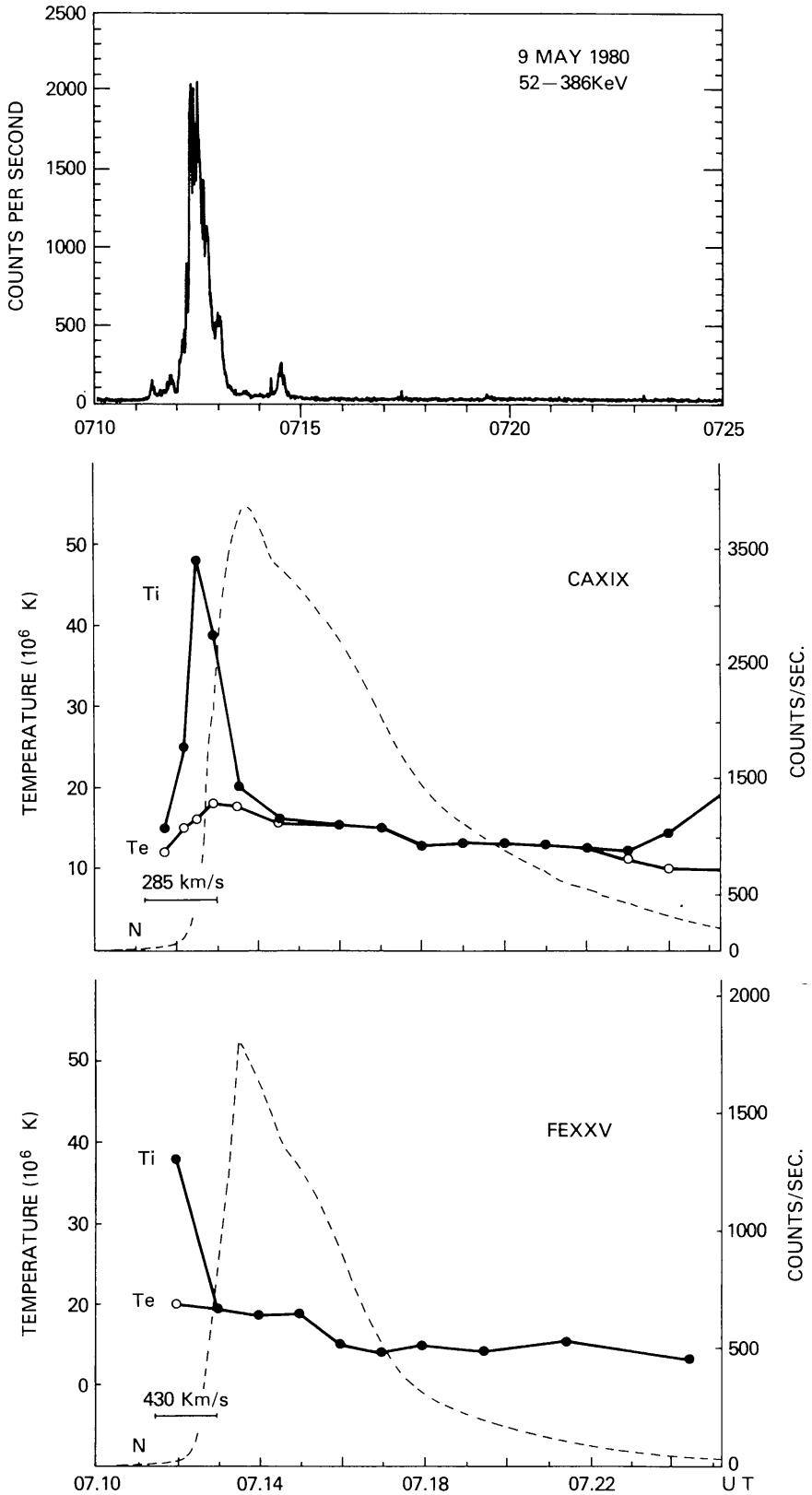

Fig. 5. Hard X-ray emission in the energy band 52-386 keV during the May 9, 1980 flare detected by the HXRBS at the top. In the middle, the time profiles of the soft X-ray emission N detected by the BCS in the Ca XIX channel, the electron temperature T_e, and the equivalent ion temperature T_i are plotted. Upwards velocities are indicated with their maximum value. At the bottom, the same parameters are derived from the Fe XXV channel.

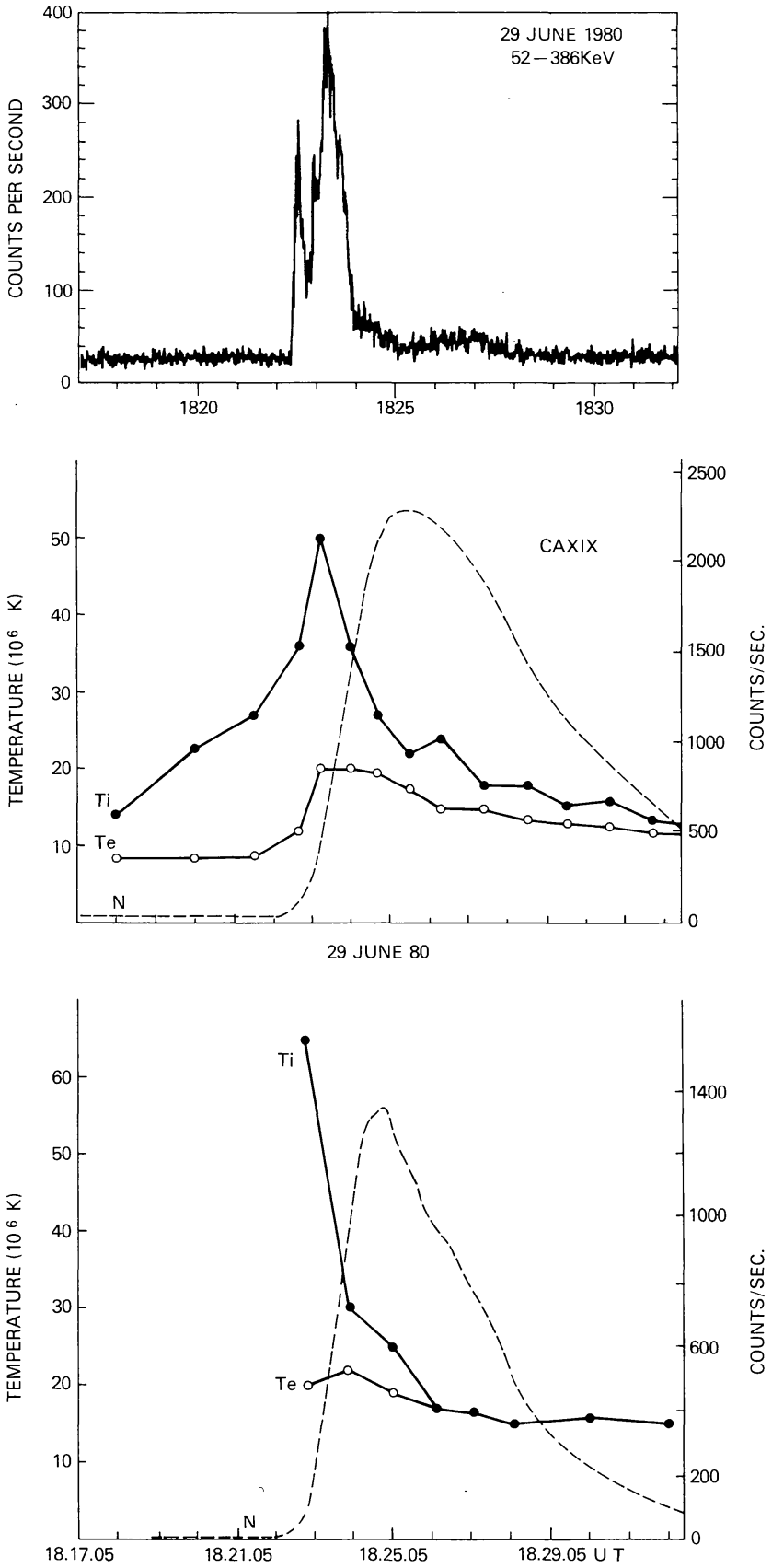

Fig. 6. The hard X-ray emission, the soft X-ray emission integrated over the Ca XIX and Fe XXV spectral regions, the electron temperature T_e and equivalent ion temperatures T_i are plotted for the June 29, 1980 flare at 18 : 22 UT.

of 9 s were used for data analysis during the hard X-ray burst). For the June 29 event (Figure 6) the pre-flare active region shows no significant turbulent motions. However, in this case the turbulent energy begins to increase a few minutes before the hard X-ray burst. Again the turbulence peaks at the hard X-ray peak.

The May 9 flare (Figure 5) reveals more clearly than the other events the existence of a period, following the impulsive phase and after the peak in the soft X-ray intensity (dashed line), during which random velocities reach their minimum value. This period lasts for several minutes. The line width of calcium lines is effectively thermal to within measurement limits in the interval from 07 : 14 to 07 : 23 UT. In the case of the other two flares this phase corresponds to a minimum turbulent velocity of approximately 40 km s^{-1}. For iron it would appear that no detectable turbulent motions are observed during the cooling phase of these flares. The nature of the bent crystal display implies that the spectrum will be convolved with the source spatial angular distribution. From the Hard X-Ray Imaging Spectrometer (HXIS) and the Flat Crystal Spectrometer (FCS) data it is known that the source size is less than 30 arc sec for these flares. This would imply a possible error in the measurements of 10% in line width or 20% in T_i, so that the differences between T_i and T_e during this minimum cannot be regarded as significant.

Later in the decay phase, turbulent motions appear to increase again to a value of approximately 60 km s^{-1} after 09 : 33 UT, 07 : 24 UT, and 18 : 41 UT, respectively for the April 10, the May 9 and the June 29 flares, although this may be due to an expansion in the source angular size. The iron emission becomes insignificant at this stage of the flare decay, so that these values are derived from the calcium decay.

The existence of these three phases: high turbulence correlated with the hard X-ray emission, minimum turbulence after the impulsive phase for several minutes, and apparent moderate turbulence (about 60 km s^{-1}) in the late decay phase is corroborated by a much wider sample of flares. The first phase is certainly associated with the impulsive phase and rapid heating in the flare region.

In addition to the characteristic broadening of the principal line profiles, a blue-shifted component is observed during the hard X-ray bursts, in all of the disk flares observed by the BCS studied up to now, including both M and X classes. The April 10 and May 9 flares are examples of this effect. During the impulsive phase of the April 10 event in the interval 09 : 17, 09 : 20 UT we observe a blue-shifted component in the calcium spectrum which indicates line of sight velocities ranging from 280 ± 30 km s^{-1} in the first minute up to 340 ± 30 km s^{-1} at the hard X-ray burst peak. Calcium spectra have been integrated over 60 s except during the peak of the hard X-ray emission during which a time integration of 9 s has been used. Line-of-sight velocities of the same order of magnitude are found for iron: 389 ± 40 km s^{-1}. Similar velocities are found for the interval 07 : 11 : 20–07 : 12 : 30 during the May 9 flare: 285 ± 30 km s^{-1} and 430 ± 40 km s^{-1} deduced respectively from calcium and iron emission.

The June 29 event is presented here as a typical example of a limb event in all of which the blue-shifted component is absent during the impulsive phase. This suggests that motions are essentially upwards; i.e. material is rising in response to the energy released

during the hard X-ray emission, probably along the field lines, with negligible horizontal velocity component. With this assumption, the magnitude of the actual upwards motion can be deduced from the line of sight components of the velocities, derived from the blue shift and the longitudinal position of the source. These corrected values of radial velocities are consistent with plasma moving at the sound speed. Corrected radial velocities are used in the following section for computing the energy flow associated with the rising material.

4. Energy Balance during the Impulsive Phase

The energy involved in the turbulent mass motions and in the upward motion of part of the hot plasma during the impulsive phase is estimated by considering the geometry and the emission measure (EM) of the source. Although the emission of the hot rising plasma is less intense than that of the principal source, the energy transported by the plasma flowing upwards is far more important than that appearing in the form of turbulent motions observed primarily in the principal source. We will analyse the energy changes involved in the April 10 flare for which the geometry is best known.

The spectral intensity observed is related to electron temperature T_e, electron density n_e and geometry of the source by

$$I = \frac{0.8hv}{4\pi L^2} A \int_V n_e^2 \frac{N_i}{N_e}(T) C(T)\, \mathrm{d}V \ \mathrm{erg\ cm^{-2}\ s^{-1}}, \tag{1}$$

where hv is the energy of the photon, L is the Earth-Sun distance, A is the element abundance, $N_i/N_e(T)$ is the ionization equilibrium function. The $C(T)$ functions are *effective* collisional excitation rate coefficients, and are the same used for constructing the theoretical spectrum of the He-like ions. We will limit our computations to the iron and calcium resonance lines, since the relative dielectronic satellite intensities are already used in deriving effective temperatures for the iron and calcium emitting regions. It is assumed that the atoms contributing to the emission, for a given element, are on the average at a temperature T_0 which is derived from the spectral intensity analysis (effectively the dielectronic satellite ratios) for each time interval. Thus the intensity can be expressed as:

$$I = \frac{0.8hv}{4\pi L^2} A \frac{N_i}{N_e}(T_0) C(T_0) \int_V n_e^2\, \mathrm{d}V = F(T_0)(EM)\,. \tag{2}$$

Steady-state ionization is justified for the comparatively slow rate of change observed, and ionization equilibrium values N_i/N_e for computing the emissivity curves $F(T)$ are those derived by Jacobs *et al.* (1980).

The emission measure for Ca XIX is computed respectively for the principal component (EM) and the blue-shifted component (EM'), whose intensity is derived from the

ratio between the principal and secondary spectral components, and using the electron temperatures plotted in Figure 4. The emission measure of the principal source increases from 4.8×10^{48} at 09 : 16 UT, pre-flare conditions, to 6.7×10^{49} at 09 : 21 : 30 UT, the highest value during the flare. The emission measure of the blue-shifted source increases from 1.4 to 3.1×10^{48} in the three minutes in which the blue-shifts are observed: 09 : 17–09 : 20 UT, and then becomes unmeasurable.

The geometry of the emitting source during the April 10 flare can be deduced from a map of the region obtained by the Flat Crystal Spectrometer (FCS), whose observations in the higher energy channels are complementary to those of the Bent Crystal Spectrometer. The FCS was scanning the flaring region in a $4' \times 4'$ raster in $15''$ steps, integrating counts at each pixel for 1.024 s. Precisely at the time of the peak of the hard X-ray burst the instrument was scanning through the bright part of the active region. The S XV and Fe XXV channels cover an energy interval which includes that of the Ca XIX photons. As it appears from the map starting at 09 : 16 : 07 UT and the subsequent one, the bright emission region was essentially contained within two consecutive pixels east-west oriented, in an area $15'' \times 30''$ for both Fe XXV and S XV. The extent of the flare is confirmed by the X-ray image in the energy range (3.5–8 keV) detected by the Hard X-ray Imaging Spectrometer (SMM) which has a spatial resolution of $8'' \times 8''$. Moreover, the April 10 event is a typical example of a flare with well-separated hard X-ray footpoints of the flaring loop, as has been discussed by Hoyng *et al.* (1981). The hard X-ray image (16–30 keV) shows that during the impulsive phase the emission is essentially confined in two pixels, $8'' \times 8''$ separated by $16''$ in the east-west direction. A hard X-ray diffuse component is also present, approximately centered between the two bright points as is the soft X-ray source. The HXIS hard X-ray emission in the bright points is temporally correlated to the integrated emission above 25 keV observed by the HXRBS. The two hard X-ray bright points can be interpreted as the sites of the energy release by a fast electron beam at the footpoints of a magnetic loop, while the primary energy release and electron acceleration occur presumably higher in the loop (Machado *et al.*, 1982).

Following the hypothesis that the blue-shifted component is due to chromospheric material heated by the energy released by electron collisions and driven up along the magnetic field lines of the loop (Canfield *et al.*, 1980) we want to test whether the ratio of the blue-shifted to the principal component, observed by the BCS, is compatible with the ratio of the X-ray emission at 3.5–8 keV in the two pixels, bright in the hard X-rays, to the total emission, observed by the HXIS. If so, the blue-shifted component can be spatially related to the sites of the energy dissipation of the electron beam. The emission measure of the rising hot material is about 0.2 of the principal source at the peak of the hard X-ray burst, in good agreement with the ratio of the footpoints to the total emission derived by the HXIS X-ray image, which is 0.26. Therefore we suggest that the principal static component of the BCS spectra is due to the soft X-ray emission integrated over the volume of the magnetic loop connecting the footpoints, while the blue-shifted component is localized in proximity of and rising from the footpoints. As a consequence the rising material should be contained in a volume V' smaller than the volume of the

total X-ray volume V, which is assumed to be 5×10^{27} cm^3 ($15'' \times 30'' \times 30''$) from the FCS observations (presumably an upper limit).

The physical parameters we have derived are sufficient for determining whether the energy and mass flows through the loop footpoints associated with the blue-shifted plasma are sufficient to justify the variation of the total energy and mass observed in the region of the flare. We assume that the blue-shifted plasma is flowing continuously, during the interval in which it is observed, through an area $A < 7 \times 10^{17}$ cm^2, corresponding to the two bright pixels in the hard X-rays images (HXIS), and that the rising material is confined in a closed magnetic configuration. In addition, we define two parameters $\alpha = V'/V$ and $\beta = T'_e/T_e$ to account for two unknown quantities, that is, the volume V' containing the blue-shifted component and its temperatures T'_e. (Although the electron temperature T_e of the principal component and T'_e were assumed equal when analysing the two component spectra, it was pointed out that only the quantity T_e was determined with sufficient accuracy.) The two unknown quantities can be determined by the continuity equations of mass and energy for the loop containing the soft X-ray plasma. It is assumed that the volume of the loop V remains constant through the flare. In what follows we have considered the physical parameters derived from the calcium emission.

A continuous increase in material in the volume of the flare is observed as long as the blue-shifted component is present ($\sim$ 3 min), consistent with the loop being filled by an evaporation process. The increase in the total electron content in the volume V during the period Δt is equal to the integral over Δt of the amount of the plasma entering the loop in unit time through the footpoints, that is:

$$\Delta N_e = \int_{\Delta t} n'_e v' A \, \mathrm{d}t \,, \tag{3}$$

where we have assumed each region to be homogeneous, so that $N_e = n_e V = \sqrt{EM}\sqrt{V}$ is the total electron number in the volume V, v' is the velocity of the plasma flowing in unit time into the loop, and $n'_e = \sqrt{EM'}/(\sqrt{\alpha}\sqrt{V})$ is the electron density of the rising plasma. The values of these quantities are tabulated in Table I. The continuity equation

TABLE I

Showing the variation with time of the various particle and energy terms on 10 April, 1980

Time interval UT	Total electron number N_e	Electron number input ($n'_e v' A$) (s^{-1})	Thermal energy E_{th} (ergs)	Turbulent energy E_{turb} (ergs)	Enthalpy input (P'_{EN}) (ergs s^{-1})	Kinetic energy input (P'_K) (ergs s^{-1})	Conduction loss P_C (ergs s^{-1})	Radiation loss P_R (ergs s^{-1})
09:15–09:17	1.5(38)	–	6.0(29)	2.4(28)	–	–	2.0(26)	2.3(26)
09:17–09:18	2.0(38)	1.5(36)	1.2(30)	3.3(28)	1.1(28)	2.3(27)	1.5(27)	3.2(26)
09:18–09:19	3.1(38)	2.6(36)	2.7(30)	8.0(28)	1.9(28)	5.4(27)	1.5(27)	7.4(26)
09:19–09:20	4.1(38)	2.6(36)	2.7(30)	8.4(28)	2.0(28)	4.7(27)	1.8(27)	1.3(27)
09:20–09:21	5.5(38)	–	3.4(30)	1.3(29)	–	–	1.5(27)	2.4(27)

(Equation (3)) leads to $\alpha \simeq 0.1$; that is, the effective volume V' in which is confined the dynamic component of the soft X-ray plasma is 0.1 times the volume of the principal source. From this we obtain that the average electron density for the blue-shifted plasma is 7×10^{10} cm^{-3}, and the evaporation process accounts for the change in density of the principal emitting source from 3×10^{10} cm^{-3} to 1.1×10^{11} cm^{-3} during the impulsive phase.

In this same interval Δt the thermal energy contained in the loop increases, reaching its maximum value at the end of the evaporation process. The variation of thermal energy during this interval is:

$$\Delta E_{\text{th}} = \Delta(3 n_e k T_e V) = \Delta(3\sqrt{EM}\sqrt{V}\, k T_e) \simeq 2 \times 10^{30} \text{ ergs} . \tag{4}$$

An additional amount of energy is accumulated during this time in the loop in the form of turbulent motions:

$$\Delta \text{E}_{\text{turb}} = \Delta(\tfrac{3}{2} m \sqrt{EM}\sqrt{V}\, v_t^2) = 8.6 \times 10^{28} \text{ ergs} , \tag{5}$$

where v_t is the turbulent velocity and m is the proton mass. The energy transported into the loop by the blue-shifted plasma, corrected for the losses due to radiative and conductive coolings can account for the total energy increase in the loop, if the following equation is satisfied:

$$\int_{\Delta t} (P'_{EN} + P'_K)\, \mathrm{d}t - \int_{\Delta t} (P_c + P_R)\, \mathrm{d}t = \Delta E_{\text{th}} + \Delta E_{\text{turb}} . \tag{6}$$

The quantities P'_{EN} and P'_k represent the enthalpy and the kinetic energy directly transported by the plasma flowing into the loop per unit time:

$$P'_{EN} = (5 k n'_e T'_e) v' A = 5 k n'_e \beta T_e v' A \quad (\text{erg s}^{-1}) , \tag{7}$$

$$P'_k = (\tfrac{1}{2} m n'_e v'^2) v' A \quad (\text{erg s}^{-1}) .$$

The radiative loss P_R is adequately derived by assuming the entire volume at the same temperature. For the range of temperatures measured during the flare we can use the approximation

$$P_R = 1.5 \times 10^{-19} n_e^2 T_e^{-1/2} V \text{ ergs s}^{-1} \tag{8}$$

(Summers and McWhirter, 1979).

The energy losses by classical heat conduction can be expressed by

$$P_c = \tfrac{2}{7} \psi T_e^{7/2} A/h \quad \text{ergs s}^{-1} , \tag{9}$$

where h is the height of the loop above the chromosphere and ψ is the coefficient of thermal conductivity. The value assumed for the height, $h \simeq 2.4 \times 10^9$ cm, is consistent with the assumption made for the volume of the region of the flare and the footpoint cross section. In Table I we report the values of the thermal and turbulent energy present in the loop as well as those of the power losses and the energy transferred into the loop during the impulsive phase. The continuity equation for the energy in the loop requires

$\beta \simeq 0.7$, that is, the electron temperature of the blue-shifted plasma would be $T'_e \simeq 12 \times 10^6$ K. However, we believe that the difference between T_e and T'_e is largely within the uncertainty in derving T'_e.

5. Discussion and Conclusion

If during the impulsive phase of the flare the soft X-ray plasma is confined in a region of approximately constant volume by the magnetic fields connecting the two footpoints, the mass and energy of the blue-shifted plasma flowing through the footpoints in this region are sufficient to account for the observed increase in mass and energy as well as for the expected energy losses due to heat conduction and radiation. This is verified if the mass and energy flow is assumed continuous during the interval in which the blue-shifted material is observed. The energy balance of the flare is described in Figure 7: the variation of the total energy of the flare (upper part of the figure) is compared with the time integrals of the energy input of the blue-shifted plasma and of the power losses by conduction and radiation (in the lower part of the figure). The total enthalpy plus

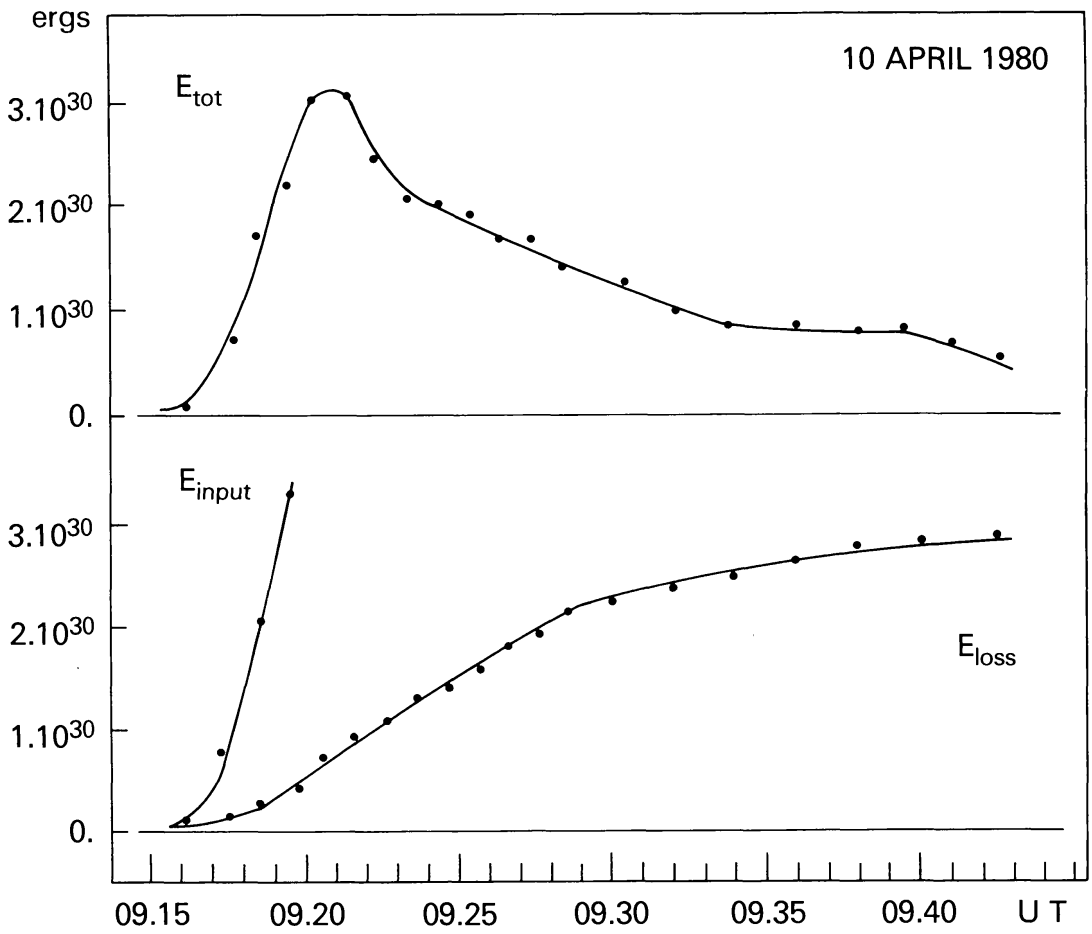

Fig. 7. In the upper part, the total energy (thermal plus turbulent energy) of the flare of April 10, 1980 is plotted. The zero level has been shifted to the preflare value, so that the energy increase during the flare can be directly read. In the lower part of the figure we have plotted at any given time t the energy entered into the loop since the beginning of the flare (E_{input}) in form of enthalpy and kinetic energy of the blue-shifted plasma and the energy lost since the beginning of the flare by conduction and radiation (E_{loss}).

kinetic energy entering the loop (3.7×10^{30} ergs) during the impulsive phase is sufficient to account for the increase in thermal and turbulent energy (3×10^{30} ergs) in the flare, whilst the difference between these quantities (7×10^{29} ergs) is consistent with our estimate of loss by conduction and radiation. This is valid on the assumption that $\beta \simeq 0.7$, that is, of approximately equal electron temperature for the plasma entering the loop and that in the loop and an electron density of $\sim 7 \times 10^{10}$ cm^{-3} for the evaporating plasma. The total energy accumulated in the flare during the impulsive phase (3×10^{30} ergs) is gradually dissipated mainly by radiation and conduction during the decay phase, since the energy lost by these two mechanisms in the interval 09:20 to 09:42 UT is $\sim 2.2 \times 10^{30}$ ergs (Figure 7) and the decrease in total energy in the same interval is $\sim 2.5 \times 10^{30}$ ergs.

It is reasonable to suggest that the turbulence observed during the impulsive phase originates during the process in which energy is accumulated in the loop. Although the turbulent energy content (8.6×10^{28} ergs) is an order of magnitude less than the total energy content, the turbulence might well be an intermediary in transferring energy from the injected plasma into random thermal motions.

It is difficult to conceive that an electron beam dissipating energy at the loop footpoints during the brief hard X-ray burst could maintain the evaporation process. The mechanism driving the upward motions starts before and lasts longer than the interval of maximum hard X-ray emission (20 s) during which the energy released by the electrons is relevant. The energy dissipated in producing the hard X-ray burst can be computed on the basis of thick target electron bremsstrahlung from the hard X-ray flux measured by the HXRBS and the HXIS instruments. At its peak the spectral index of the hard X-rays is $\gamma \simeq 5.5$ and the flux of the photons with energies greater than 20 keV is $I(20) \simeq 25$ photon cm^{-2} s^{-1} keV^{-1}. Assuming that the impact electrons at the footpoints of the loop are $\frac{2}{3}$ of the total emission, the power dissipated by the electrons is $P = 2.8 \times 10^{28}$ erg s^{-1} (Machado *et al.*, 1982). The energy (5.6×10^{29} ergs) dissipated in 20 s, the interval of maximum hard X-ray emission, may not be sufficient to account for the total energy carried by the blue-shifted component during the impulsive phase of 3.7×10^{30} ergs, although the error in this estimate may be large. This supports the hypothesis that during the impulsive phase of the flare, over a period of several minutes, an energy input is required, additional to that indicated by the hard X-ray burst, in order to maintain the chromospheric evaporation observed.

Acknowledgements

The work reported has benefited from important discussions and contributions from many other members of the XRP team, in particular C. J. Wolfson and K. J. H. Phillips. We thank also J. Dubau for contributions to the spectral fitting procedures. We wish to acknowledge assistance from K. J. Frost of the HXRBS team and D. M. Speich of NOAA. E. Antonucci was supported on a Fellowship from ESA, and on SAS Contract No. 80/0164.

References

Acton, L. W., Culhane, J. L., Gabriel, A. H., Bentley, R. D., Bowles, J. A., Firth, J. G., Finch, M. L., Gilbreth, C. W., Guttridge, P., Hayes, R. W., Joki, E. G., Jones, B. B., Kent, B. J., Leibacher, J. W., Nobles, R. A., Patrick, T. J., Phillips, K. J. H., Rapley, C. G., Sheather, P. H., Sherman, J. C., Stark, J. P., Springer, L. A., Turner, R. F., and Wolfson, C. J.: 1980, *Solar Phys.* **65**, 53.

Bhalla, C. P., Gabriel, A. H., and Presnyakov, L. P.: 1975, *Monthly Notices Roy. Astron. Soc.* **172**, 359.

Bely-Dubau, F., Gabriel, A. H., and Volonté, S.: 1979a, *Monthly Notices Roy. Astron. Soc.* **189**, 802.

Bely-Dubau, F., Gabriel, A. H., and Volonté, S.: 1979b, *Monthly Notices Roy. Astron. Soc.* **186**, 405.

Bely-Dubau, F., Dubau, J., Faucher, P., and Gabriel, A. H.: 1982, *Monthly Notices Roy. Astron. Soc.*, (in press).

Bely-Dubau, F., Dubau, J., Faucher, P., Gabriel, A. H., Loulergue, M., Steenman-Clark, L., Volonté, S., Antonucci, E., and Rapley, C. G.: 1982, in preparation.

Canfield, R. C., Brown, J. C., Brueckner, G. E., Cook, J. W., Craig, I. J. D., Doschek, G. A., Emslie, A. G., Henoux, J. C., Lites, B. W., Machado, M. E., and Underwood, J. H.: 1980, *Solar Flares*, Skylab Solar Workshop II, p. 231.

Culhane, J. L., Gabriel, A. H., Acton, L. W., Rapley, C. G., Phillips, K. J., Wolfson, C. J., Antonucci, E., Bentley, R. D., Catura, R. C., Jordan, C., Kayat, M. A., Kent, B. J., Leibacher, J. W., Parmar, A. N., Sherman, J. C., Springer, L. A., Strong, K. T., and Veck, N. J.: 1981, *Astrophys. J. Letters* **244**, L141.

Doschek, G. A., Feldman, U., Kreplin, R. W., and Cohen, L.: 1980, *Astrophys. J. Letters* **239**, 725.

Feldman, V., Doscheck, G. A., Kreplin, R. W., and Mariska, J. T.: 1980, *Astrophys. J. Letters* **241**, 1175.

Gabriel, A. H.: 1972, *Monthly Notices Roy. Astron. Soc.* **160**, 99.

Gabriel, A. H., Acton, L. W., Culhane, J. L., Phillips, K. J. H., Wolfson, C. J., Rapley, C. G., Antonucci, E., Bentley, R. D., Jordan, C., Kayat, M. A., Leibacher, J. W., Levay, M., Sherman, J. C., Strong, K. T., and Veck, N. J.: 1981a, *Astrophys. J. Letters* **244**, L147.

Gabriel, A. H., Culhane, J. L., Acton, L. W., Antonucci, E., Bentley, R. D., Jordan, C., Leibacher, J. W., Parmar, A. N., Phillips, K. J. H., Rapley, C. G., Wolfson, C. J., and Strong, K. T.: 1981b, *Cospar Proceedings*, Adv. Space Res. No. 1, p. 267.

Hoyng, P., Duijveman, A., Machado, M. E., Rust, D. M., Švestka, Z., Boelee, A., De Jager, C., Frost, K. J., Lafleur, H., Simnelt, G. M., van Beek, H. F., and Woodgate, B. E.: 1981, *Astrophys. J. Letters* **246**, L155.

Jacobs, V. L., Davis, J., Rogerson, J. E., Blaha, M., Cain, J., and Davis, M.: 1980, *Astrophys. J. Letters* **239**, 1119.

Machado, M. E., Duijveman, and Dennis, B. R.: 1982, *Solar Phys.*, (in press).

Summers, H. P. and McWhirter, P.: 1979, *J. Phys.* **B12**, 2387.